Protease-activated receptor 1 activation enhances doxorubicin-induced cardiotoxicity

Silvio Antoniak[a,b,*], Kohei Tatsumi[a,c], Clare M. Schmedes[a], Steven P. Grover[a], Rafal Pawlinski[a], Nigel Mackman[a]

[a] Department of Medicine, Thrombosis and Hemostasis Program, Division of Hematology and Oncology, UNC McAllister Heart Institute, University of North Carolina, Chapel Hill, NC, United States

[b] Department of Pathology and Laboratory Medicine, University of North Carolina at Chapel Hill, Chapel Hill, NC, United States

[c] Department of Physiology and Regenerative Medicine, Kindai University, Faculty of Medicine, Osaka-sayama, Osaka, Japan

ARTICLE INFO

Keywords:
Protease-activated receptor 1
Doxorubicin
Heart failure
Vorapaxar

ABSTRACT

Objective: The anti-cancer anthracycline drug Doxorubicin (Dox) causes cardiotoxicity. We investigated the role of protease-activated receptor 1 (PAR-1) in Dox-induced cardiotoxicity.

Methods and results: In vitro experiments revealed that PAR-1 enhanced Dox-induced mitochondrial dysfunction, reactive oxygen species and cell death of cardiac myocytes and cardiac fibroblasts. The contribution of PAR-1 to Dox-induced cardiotoxicity was investigated by subjecting PAR-1$^{-/-}$ mice and PAR-1$^{+/+}$ mice to acute and chronic exposure to Dox. Heart function was measured by echocardiography. PAR-1$^{-/-}$ mice exhibited significant less cardiac injury and dysfunction compared to PAR-1$^{+/+}$ mice after acute and chronic Dox administration. PAR-1$^{-/-}$ mice had reduced levels of nitrotyrosine, apoptosis and inflammation in their heart compared to PAR-1$^{+/+}$ mice. Furthermore, inhibition of PAR-1 in wild-type mice with vorapaxar significantly reduced the acute Dox-induced cardiotoxicity.

Conclusion: Our results indicate that activation of PAR-1 contributes to Dox-induced cardiotoxicity. Inhibition of PAR-1 may be a new approach to reduce Dox-induced cardiotoxicity in cancer patients.

1. Introduction

The anthracycline antibiotic Doxorubicin (Dox) is a very effective anti-cancer agent that is widely used in the treatment of breast cancer, lymphoma, leukemia, and sarcomas [1]. However, Dox induces cardiovascular complications either very early after the first injection or years after completion of chemotherapy [1]. The most common complications of Dox cardiotoxicity are left ventricular dysfunction, myocardial ischemia, conduction disturbances, arrhythmias, hypertension, and venous thromboembolism. The incidence of these cardiovascular complications can reach up to 28% of treated patients, which is dependent on the dose, duration and combination with other anti-cancer drugs [1, 2].

The major mechanism by which Dox induces heart failure involves disruption of DNA and RNA synthesis, oxidative damage via the formation of reactive oxygen species (ROS), changes in mitochondrial membrane potential $\Delta\Psi m$, apoptosis, as well as necrosis of cardiac myocytes (CMs) [2–4]. CMs are highly susceptible to Dox because of their high metabolic rate, their limited ability to handle oxidative stress and their low rate of replication. Importantly, Dox-mediated injuries are permanent. Dox-induced cardiotoxicity still occurs even with the current anti-cancer regimes. Indeed, cardiac injury induced by cancer therapy is a significant problem and is studied in the new field of cardio-oncology [2, 5].

Protease-activated receptor 1 (PAR-1) is a G-protein coupled receptor that is expressed in the heart by CMs and cardiac fibroblasts (CFs) [6–8]. In contrast to human platelets, PAR-1 is not expressed on mouse platelets. PAR-1 activation increases vascular permeability, leukocyte recruitment and expression of inflammatory mediators [9, 10]. We have found that PAR-1 contributes to cardiac injury. For instance, we found that PAR-1$^{-/-}$ mice had reduced cardiac remodeling after ischemia-reperfusion injury [6, 11, 12]. In addition, PAR-1$^{-/-}$ mice had reduced perivascular fibrosis and heart failure in an angiotensin II infusion model [13]. Chemotherapy is often associated with the activation of coagulation that is mediated by either an increase in tissue factor (TF) activity on tumor cells due to increased exposure of the negatively-charged phospholipid phosphatidylserine (TF de-encryption), or the induction of TF expression within the vasculature

* Corresponding author at: University of North Carolina at Chapel Hill, 111 Mason Farm Road, Campus Box 7126, Chapel Hill, NC 27599, United States.
E-mail address: antoniak@email.unc.edu (S. Antoniak).

https://doi.org/10.1016/j.yjmcc.2018.08.008
Received 13 February 2018; Received in revised form 7 August 2018; Accepted 9 August 2018
Available online 10 August 2018

[14–16]. In addition, Dox increases the permeability of the endothelium, which would allow access of circulating clotting factors to TF in the vessel wall and tissues, such as the heart [6, 17, 18]. Indeed, PAR-1 is the primary receptor for thrombin but can be activated by other proteases, such as matrix metalloproteinase (MMP) [6, 19, 20].

In this study, we investigated the role of PAR-1 in Dox-induced cardiotoxicity using in vitro and in vivo models.

2. Material and methods

2.1. Isolation and culture of cardiac cells

Rat CFs and CMs were isolated from one-day old rat neonates using a commercial kit (Worthington Biochemical Corporation, Lakewood, NJ) [21]. Mouse CFs and CMs were isolated from embryos (E14) from PAR-1$^{+/+}$ and PAR-1$^{-/-}$ mice and cultured as described [22, 23]. Cells were incubated with 1 μM Dox in FBS-free media which is similar to the plasma concentrations in patients [24]. In addition, cells were stimulated with 150 μM of a PAR-1 agonist peptide (AP) or scrambled control peptide (Abgent, San Diego, CA) [22, 25].

2.2. Measurement of cardiac troponin-I, protein nitrotyrosine, acetylated p53, CXCL1 and myeloperoxidase

Cardiac and cardiac myocyte injury were quantified by measuring levels of cardiac troponin-I by ELISA (Life Diagnostics, West Chester, PA) in plasma and culture supernatant, respectively, as described [26]. A commercial ELISA was used to measure levels of nitrotyrosine in protein (Hycult, Plymouth Meeting, PA). Acetylation of p53, as marker for apoptosis, was measured with the PathScan® Acetylated p53 Sandwich ELISA Kit (Cell Signaling, Danvers, MA). CXCL1 and myeloperoxidase protein levels in heart lysates were analyzed using a Duo-Set® (R&D Systems) [25]. All assays were performed according to the manufacturers' instructions.

2.3. Measurement of cell viability

Cell membrane integrity was analyzed using SYTOX® Green nucleic acid stain. SYTOX green penetrates compromised cell membranes and binds to DNA. Fluorescence of DNA-bound SYTOX® Green was detected at 504/523 nm. Viability of cultured cells was analyzed using Alamar Blue® (Invitrogen, Carlsbad, CA). Cells were incubated for 2 h after stimulation with Alamar Blue® according to the manufacture's instruction and the fluorescence measured in a plate reader (SpectraMax M5, Molecular Devices).

2.4. Measurement of mitochondrial membrane potential ΔΨm

The fluorescent dye 5,5′,6,6′-Tetrachloro-1,1′,3,3′-tetraethylbenzimidazolocarbocyanine iodide (JC-1; R&D Systems, Minneapolis, MN) accumulates in mitochondria in a potential-dependent manner and was employed to detect changes in mitochondrial membrane potential (ΔΨm) [3]. Cells were stained with JC-1 (7 μM in PBS) for 15 min in the dark at 37 °C, washed once and the fluorescence was measured at 595/525 nm with a SpectraMax M5 plate reader (Molecular Devices, Sunnyvale, CA). To inhibit intracellular Ca^{2+} signaling, cells were incubated with BAPTA-AM (10 μM, Sigma-Aldrich, St. Louis, MO) or vehicle one hour before treatment.

2.5. Measurement of ROS

CFs and CMs were incubated with Dox and/or PAR-1 AP for indicated time points. Next, cells were stained with 20 μM 2′,7′–dichlorofluorescin diacetate (DCFDA, Sigma-Aldrich) 90 min prior to analysis. For this, conditioned media was temporarily removed and stored in cell incubator. Pre-warmed FBS-free DMEM supplemented with DCF or DMSO vehicle was added to the cells for 30 min. Stained cells were washed in pre-warmed FBS-free DMEM and cells incubated with conditioned media for 60 min. Then, cells were washed and stored on ice until the final 2′, 7′–dichlorofluorescein (DCF) fluorescence measurement. Signals were normalized with the fluorescence of DMSO stained cells. Mitochondrial superoxide generation was analyzed by with the MitoSOX™ Red mitochondrial superoxide indicator. Cells were incubated with 2.5 μM MitoSOX™ for 10 min at 37 °C, washed 3 times and the fluorescence detected at 510/580 nm.

2.6. Western blot

CFs and CMs cell lysates were supplemented with 4× loading buffer, boiled for 7 min and subjected to 4–20% Mini-PROTEAN TGX gel electrophoresis (BioRad) to separate proteins [22]. Next, proteins were blotted onto a PVDF membrane, blocked with protein-free blocking buffer (Thermo Fisher Scientific, Waltham, MA) and incubated overnight at 4 °C with the primary antibodies against cleaved PARP at Asp214 (D6X6X, 1:1000, Cell Signaling), BAX (D3R2M, 1:1000, Cell Signaling), BCL2 (D17C4, 1:1000, Cell Signaling) or glyceraldehyde 3-phosphate dehydrogenase (GAPDH, L-18, 1:10000, Santa Cruz Biotechnology). Primary antibodies were visualized on washed membranes with fluorescence labeled secondary antibodies (1:10000) for 1 h and analyzed using an Odyssey Infrared System (LI-COR Bioscience, Lincoln, NE) [22]. Signal intensities were analyzed using Image J 1.43u (National Institutes of Health, Bethesda, MD).

2.7. Acute and chronic mouse models of Dox-induced cardiotoxicity

We used male PAR-1$^{+/+}$ (wild-type [WT]) and PAR-1$^{-/-}$ mice (8–12 weeks old) on a C57Bl/6 J background [27]. Both mouse lines were kept as cousin lines. Acute Dox cardiotoxicity was induced in mice with a single intraperitoneal (i.p.) dose of Dox (20 mg/kg body weight) and cardiac function was evaluated after 5 days [4]. Chronic Dox cardiotoxicity was induced in mice by injecting Dox (5 mg/kg body weight) weekly i.p. for 5 weeks to reach a cumulative dose of 25 mg/kg body weight after 35 days [28]. PAR-1 was inhibited by daily oral gavage of WT mice with vorapaxar (SCH530348, 30 μg/kg in 20% DMSO/80% saline solution, Axon, Reston, VA). Blood was collected from the inferior vena cava and plasma prepared as described [29]. Tissue was snap frozen in liquid nitrogen and stored at −80 °C [26, 30]. The study was performed in accordance with the guidelines of the animal care and use committee of the UNC at Chapel Hill and complies with National Institutes of Health guidelines.

3. Echocardiography

Echocardiography was performed on conscious mice before and after Dox treatment using a VisualSonics Vevo 2100 ultrasound system as described [13]. Left ventricle (LV) function was measured by M-mode echocardiography in the short-axis view at the mid-ventricular level. The percentage of fractional shortening was assessed by measuring the end-diastolic and end-systolic diameter [(end-diastolic diameter–end-systolic diameter)/end-diastolic diameter × 100 (%)]. Echocardiography recording and analysis were performed in a blinded fashion.

3.1. Statistical analysis

GraphPad Prism 5.01 (GraphPad Software Inc., La Jolla, CA) was used for all statistical analysis. Data are represented as mean ± SEM. For multiple-group comparison, normally distributed data were analyzed by 1- or 2-way ANOVA tests and were Bonferroni-corrected for repeated measures over time. A P-value ≤ .05 was regarded as significant.

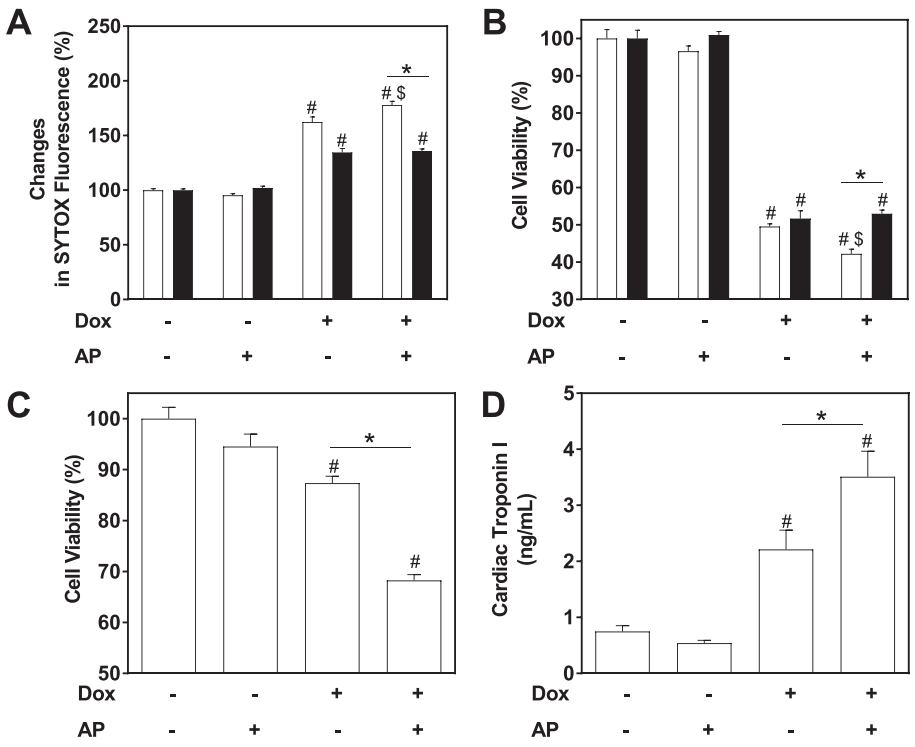

Fig. 1. PAR-1 activation increases cell injury and death of cardiac myocytes after treatment with doxorubicin. Cardiac myocytes (CMs) were incubated with 1 μM doxorubicin (Dox) and/or 150 μM PAR-1 AP. A: Cell membrane integrity of PAR-1$^{+/+}$ (white bars) and PAR-1$^{-/-}$ (black bars) mouse CMs was analyzed with SYTOX® Green after 24 h stimulation. B: Cell viability of PAR-1$^{+/+}$ (white bars) and PAR-1$^{-/-}$ (black bars) mouse CMs after 24 h stimulation was determined using AlamarBlue®. C: Cell viability of rat CMs treated with Dox and/or PAR-1 AP for 48 h was determined using AlamarBlue®. D: Release of cardiac troponin I into the media from rat CMs treated with Dox and/or PAR-1 AP for 48 h. Data (mean ± SEM; n = 4–9 per group) were analyzed by 2-way (A and B) and 1-way (C and D) ANOVA. $^{*}P < .05$, $^{\#}P < .05$ vs. control within the same genotype, $^{\$}P < .05$ vs. Dox alone within the same genotype.

4. Results

4.1. PAR-1 activation enhances Dox-induced cell injury and death of CMs

Mouse CMs from PAR-1$^{+/+}$ and PAR-1$^{-/-}$ mice embryos (E14) were treated with Dox (1 μM) and/or PAR-1 AP (150 μM) and cell membrane injury and viability were analyzed. PAR-1 activation alone did not affect cell membrane permeability for the SYTOX® Green stain but significantly increased Dox-induced cell membrane permeability of mouse embryonic PAR-1$^{+/+}$ but not PAR-1$^{-/-}$ CMs (Fig. 1A). Furthermore, PAR-1 activation alone had no effect on mouse CM viability measured by AlamarBlue® but significantly increased Dox-induced cell death of mouse CMs (Fig. 1B). Similarly, PAR-1 activation did not affect cell viability but significantly increased Dox-induced cell death of rat CMs measured by AlamarBlue® (Fig. 1C). In addition, PAR-1 stimulation significant increased Dox-induced cardiac troponin I release from rat CMs (Fig. 1D).

Similar to the results with mouse CMs, PAR-1 activation alone did not affect cell membrane integrity but significantly increased Dox-induced cell membrane permeability for the SYTOX® Green dye of mouse embryonic PAR-1$^{+/+}$ but not PAR-1$^{-/-}$ CFs (Fig. 2A). Furthermore, PAR-1 activation alone had no effect on mouse embryonic CFs viability but significantly increased Dox-induced reduction of cell viability of mouse CFs analyzed by AlamarBlue® (Fig. 2B).

4.2. PAR-1 activation enhances Dox-induced mitochondrial dysfunction in CMs

Dox has been shown to reduce ΔΨm [3, 4, 31]. Dox-induced mitochondrial dysfunction is associated with increased oxidative stress and ROS formation, including mitochondrial superoxide generation. We measured mitochondrial function in PAR-1$^{+/+}$ and PAR-1$^{-/-}$ embryonic mouse CMs using the JC-1 staining method after incubation with Dox (1 μM) and/or PAR-1 activation (150 μM PAR-1 AP) for 16 h [3]. PAR-1 activation alone had no effect on the ΔΨm in mouse CMs of both genotypes but significantly increased Dox-induced mitochondrial dysfunction (Fig. 3A). Next, we visualized the generation of ROS using the DCF staining method after incubating PAR-1$^{+/+}$ and PAR-1$^{-/-}$ embryonic mouse CMs with Dox and/or PAR-1 AP for 6 h. Again, PAR-1 activation did not affect intracellular ROS formation but increased Dox-induced ROS generation only in PAR-1$^{+/+}$ CMs (Fig. 3B). Furthermore, PAR-1 activation resulted in an increase in mitochondria specific

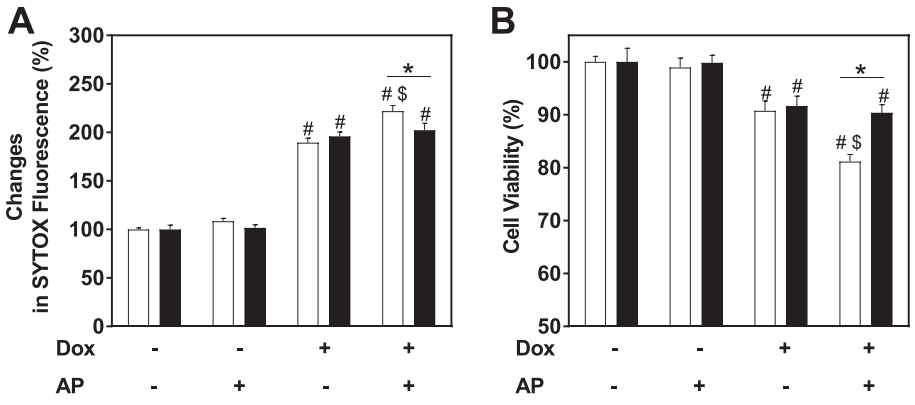

Fig. 2. PAR-1 activation increases cardiac fibroblast cell injury and death after treatment with doxorubicin. Mouse cardiac fibroblasts (CFs) were incubated with 1 μM doxorubicin (Dox) and/or 150 μM PAR-1 AP. A: Cell membrane integrity of PAR-1$^{+/+}$ (white bars) and PAR-1$^{-/-}$ (black bars) mouse CFs was analyzed with SYTOX® Green after 24 h stimulation. B: Cell viability of PAR-1$^{+/+}$ (white bars) and PAR-1$^{-/-}$ (black bars) mouse CFs was determined with AlamarBlue® after 24 h stimulation. Data (mean ± SEM; n = 5–9 per group) were analyzed by 2-way ANOVA. $^{*}P < .05$, $^{\#}P < .05$ vs. control within the same genotype, $^{\$}P < .05$ vs. Dox alone within the same genotype.

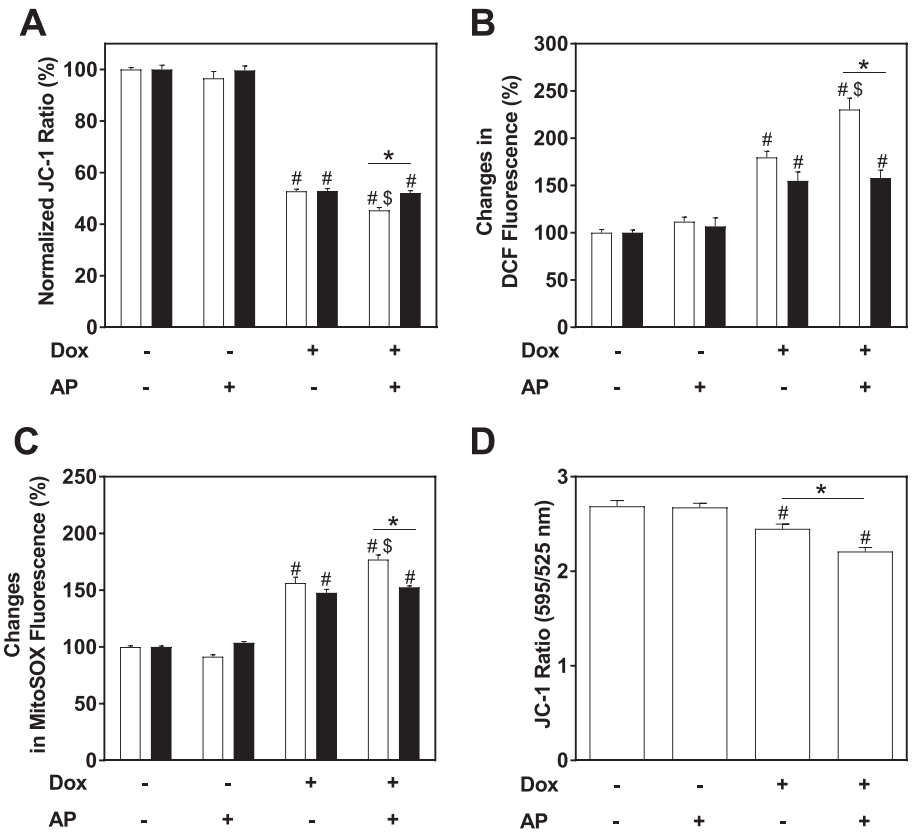

Fig. 3. PAR-1 activation reduces mitochondrial membrane potential ΔΨm and increases oxidative stress in cardiac myocytes treated with doxorubicin. Cardiac myocytes (CMs) isolated from PAR-1$^{+/+}$ (white bars) and PAR-1$^{-/-}$ (black bars) mouse hearts (A–C) and rat hearts (D) were incubated with 1 μM doxorubicin (Dox) and/or 150 μM PAR-1 AP. A: Changes in the mitochondrial membrane potential $\Delta\psi_m$ was analyzed after stimulation for 16 h using the JC-1 staining method in mouse CMs. JC-1 595/525 nm ratios of the respective unstimulated controls were set to 100. B: Generation of reactive oxygen species in mouse CMs was analyzed using the DCF method after 6 h of Dox and/or PAR-1 AP stimulation. C: Changes in mitochondrial superoxide levels were measured in mouse CMs using the MitoSOX™ staining method. D: Mitochondrial membrane potential $\Delta\psi_m$ was measured via JC-1 staining in rat CMs after 16 h of stimulation. Data (mean ± SEM; n = 5–9 per group) were analyzed by 2-way (A–C) and 1-way (D) ANOVA. $^{*}P < .05$, $^{\#}P < .05$ vs. controls of respective genotype or treatment. $^{\$}P < .05$ vs. Dox alone within the same genotype.

superoxide generation in Dox-treated PAR-1$^{+/+}$ CMs after 16 h (Fig. 3C). In addition, rat neonatal CMs showed similar PAR-1 dependent ΔΨm changes during Dox treatment (Fig. 3D). Again, PAR-1 AP (150 μM) did not affect ΔΨm but significantly reduced Dox-mediated ΔΨm changes after 16 h of stimulation (1 μM Dox) (Fig. 3D).

4.3. PAR-1 activation enhances Dox-induced mitochondrial dysfunction in CFs

Changes in ROS and mitochondrial superoxide generation were analyzed in PAR-1$^{+/+}$ and PAR-1$^{-/-}$ embryonic mouse CFs 6 and 16 h after treatment with 1 μM Dox and/or 150 μM PAR-1 AP, respectively. Similar to mouse CMs, PAR-1 activation did not change ROS (Fig. 4A) or superoxide (Fig. 4B) generation. However, PAR-1 activation significantly increased Dox-induced ROS (Fig. 4A) and superoxide levels (Fig. 4B) in PAR-1$^{+/+}$ but not PAR-1$^{-/-}$ embryonic mouse CFs. Next, we used rat CFs to analyze the effect of PAR-1 stimulation on ΔΨm. Again, PAR-1 AP (150 μM) had no effect on the JC-1 ratio (Fig. 4C) but significantly decreased Dox-induced depression of ΔΨm after 16 h of incubation with 1 μM Dox (Fig. 4C).

PAR-1 activation induces Ca^{2+}-dependent signaling [20]. Thus, we pre-treated rat CFs with BAPTA (10 μM) to analyze if the observed PAR-1 effect on ΔΨm in rat CFs after Dox incubation was Ca^{2+}-dependent. BAPTA and/or PAR-1 stimulation had no effect on ΔΨm (Fig. 4D). Importantly, inhibition of Ca^{2+}-dependent signaling abolished the PAR-1-dependent reduction in ΔΨm in rat CFs treated with Dox and PAR1 AP (Fig. 4D).

4.4. PAR-1 stimulation increases Dox-induced apoptosis in mouse CMs and CFs

To analyze the effect of PAR-1 activation on Dox-induced apoptosis, we performed Western blot analysis to detect PARP cleavage at Asp214. PAR-1$^{+/+}$ and PAR-1$^{-/-}$ mouse CMs (Fig. 5A) and CFs (Fig. 5B) were incubated with Dox (1 μM) and/or PAR-1 AP (150 μM) for 24 h and cleaved PARP protein levels were analyzed. PAR-1 activation had no effect on PARP cleavage in CMs of both genotypes but increased Dox-induced PARP cleavage in PAR-1$^{+/+}$ but not PAR-1$^{-/-}$ embryonic mouse CMs (Fig. 5A). Interestingly, PAR-1$^{+/+}$ embryonic mouse CFs showed a significant increase in PARP cleavage when stimulated with PAR-1 AP alone compared to PAR-1$^{-/-}$ CFs (Fig. 5B). In addition, PAR-1 AP further increased Dox-induced PARP cleavage in PAR-1$^{+/+}$ CFs but not PAR-1$^{-/-}$ embryonic mouse CFs (Fig. 5B).

4.5. Effect of PAR-1 deficiency on Dox-induced oxidative stress, markers of apoptosis, cardiac injury and impairment of cardiac function

We used both the acute (5 days) and chronic (35 days) mouse models of Dox-induced cardiotoxicity [4]. Dox increases cardiac injury due to oxidative stress, inflammation, apoptotic and necrotic processes within the heart [32, 33]. We analyzed the protein expression of the apoptosis regulators BAX (pro-apoptotic marker) and BCL2 (anti-apoptotic marker) before and after Dox injection in PAR-1$^{+/+}$ and PAR-1$^{-/-}$ mice hearts (Supplement figure). An increased in the BAX:BCL2 ratio is associated with a more apoptotic phenotype of cells and tissues [34]. We observed comparable BAX:BCL2 protein ratios in both genotypes before Dox injection (Fig. 6A). Importantly, the BAX:BCL2 protein ratio in hearts of PAR-1$^{-/-}$ mice was significantly lower compared to PAR-1$^{+/+}$ mice after Dox injection (Fig. 6A). An increased apoptotic phenotype can also be determined by measuring PARP cleavage in heart lysates. Again, we did not see any differences in PARP cleavage at baseline (Fig. 6B). However, PARP cleavage was higher in the hearts of Dox-treated PAR-1$^{+/+}$ mice compared to PAR-1$^{-/-}$ mice (Fig. 6B). Next, we assessed oxidative stress by measuring nitrotyrosine modification of proteins in the hearts of PAR-1$^{+/+}$ and PAR-1$^{-/-}$ mice after Dox injection. PAR-1$^{-/-}$ exhibited significant less nitrotyrosine of proteins 5 days after injection compared with PAR-1$^{+/+}$ mice (Fig. 6C). Acetylation of p53 is a marker for p53-dependent

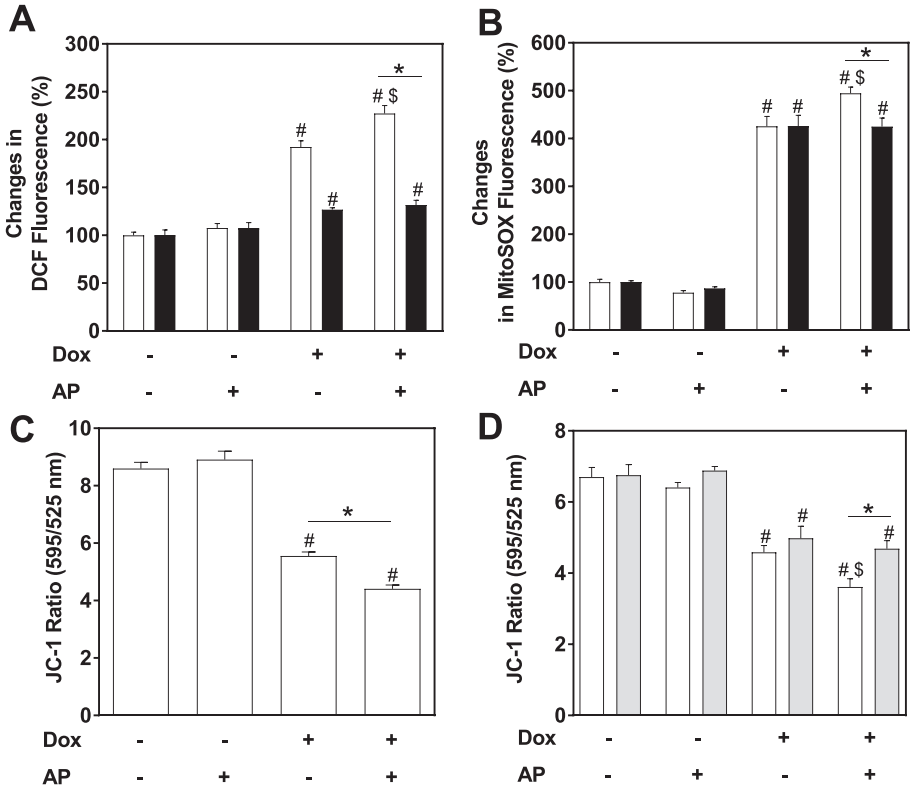

Fig. 4. PAR-1 activation increases oxidative stress and reduces mitochondrial membrane potential ΔΨm and in cardiac fibroblasts treated with doxorubicin. Cardiac fibroblasts (CFs) isolated from PAR-$1^{+/+}$ (white bars) and PAR-$1^{-/-}$ (black bars) mouse hearts (A, B) and rat hearts (C, D) were incubated with 1 μM doxorubicin (Dox) and/or 150 μM PAR-1 AP. A: Generation of reactive oxygen species in mouse CFs was analyzed using the DCF method after 6 h of Dox and/or PAR-1 AP stimulation. B: Changes in mitochondrial superoxide levels were measured in mouse CFs using the MitoSOX™ staining method. C: Mitochondrial membrane potential $\Delta\psi_m$ was measured via JC-1 staining in rat CFs after 16 h of stimulation. D: Changes in the JC-1 ratio in rat CFs with the Ca^{2+} chelator (BAPTA, 10 μM, gray bars) or vehicle control (white bars) after incubation with 1 μM Dox (Dox) and/or 150 μM PAR-1 AP for 16 h. Data (mean ± SEM; n = 5–9 per group) were analyzed by 2-way (A, B, D) and 1-way (C) ANOVA. $^{*}P < .05$, $^{\#}P < .05$ vs. controls of respective genotype or treatment. $^{\$}P < .05$ vs. Dox alone within the same genotype.

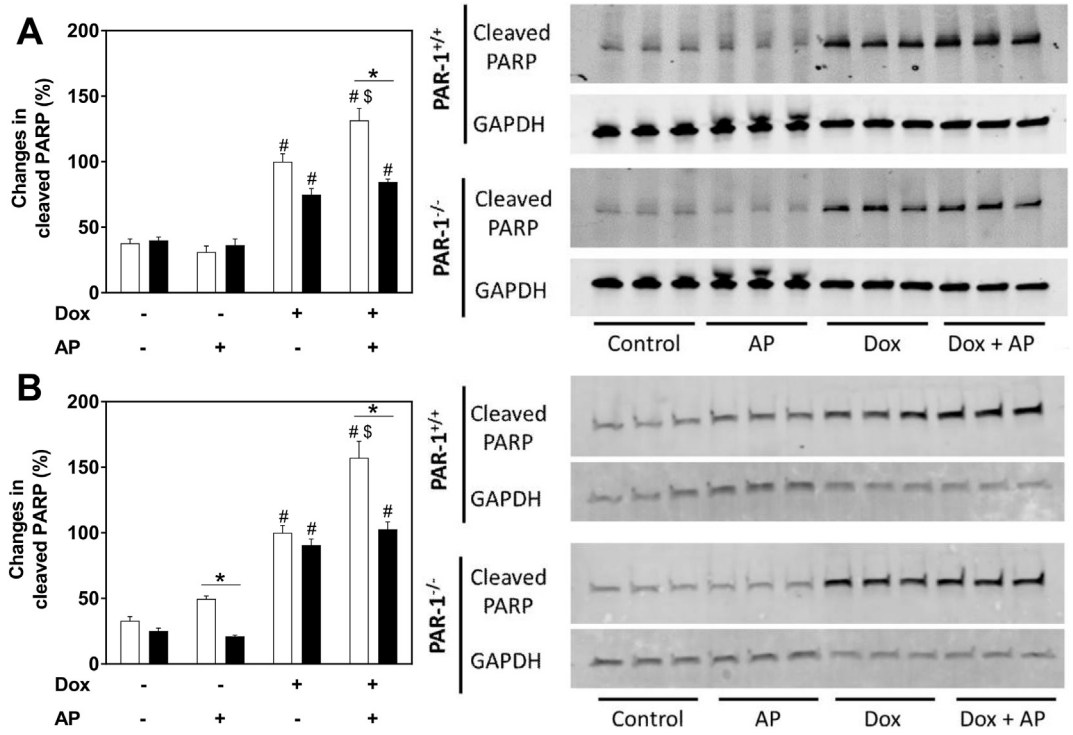

Fig. 5. PAR-1 activation increases apoptosis in cardiac myocytes and cardiac fibroblasts treated with doxorubicin. Mouse cardiac myocytes (CMs) and cardiac fibroblasts (CFs) from PAR-$1^{+/+}$ (white bars) and PAR-$1^{-/-}$ (black bars) mouse hearts were stimulated with 1 μM Doxorubicin (Dox) and/or 150 μM PAR-1 AP for 24 h. Quantifications and representative Western blots of PARP cleavage at Asp214 (89 kDa fragment) of CMs (A) and CFs (B). Cleaved PARP levels of the Dox alone group in PAR-$1^{+/+}$ were set to 100. GAPDH (39 kDa) protein levels were used as loading control. Data (mean ± SEM; $n = 3$–6 per proup) were analyzed by 2-way ANOVA. $^{*}P < .05$, $^{\#}P < .05$ vs. controls. $^{\$}P < .05$ vs. Dox alone within the same genotype.

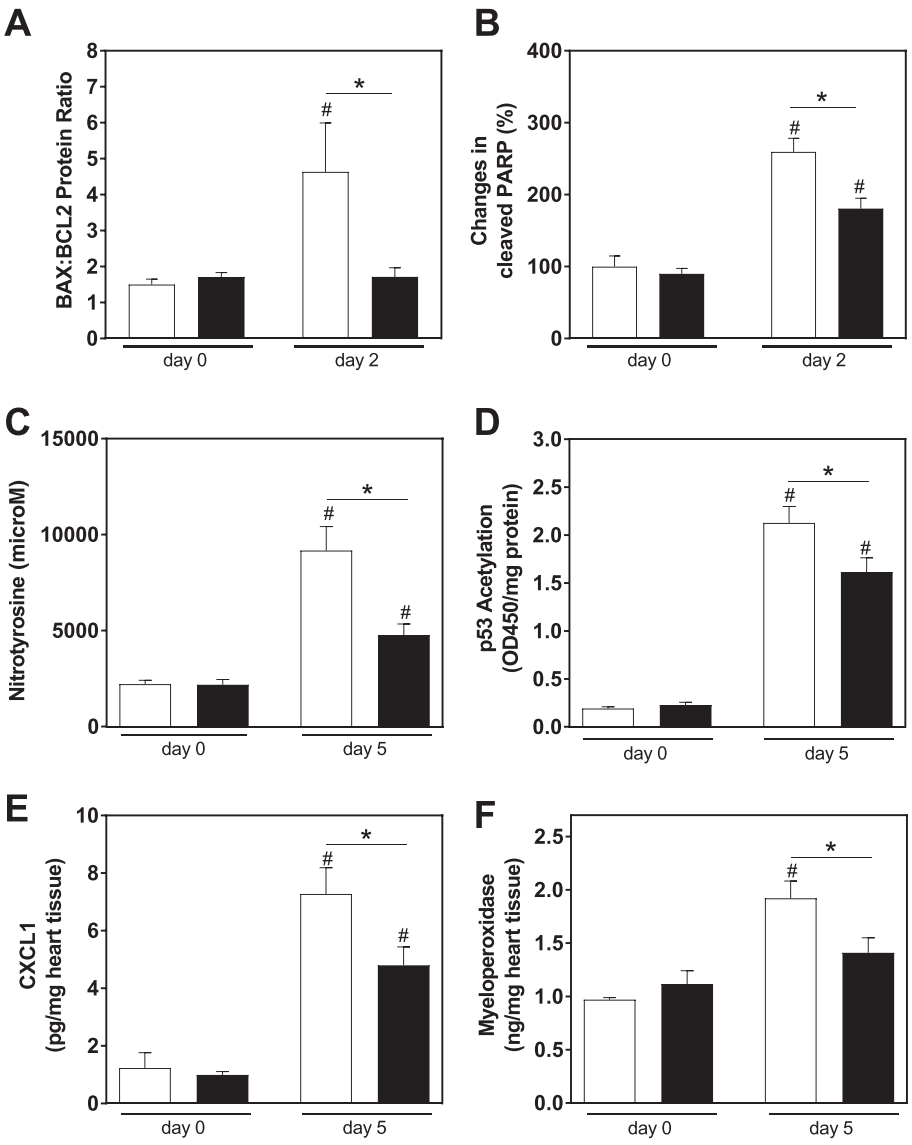

Fig. 6. PAR-1 deficiency is associated with reduced oxidative stress, apoptosis and inflammation in the heart after doxorubicin injection. Heart samples were collected from PAR-$1^{+/+}$ (white bar) and PAR-$1^{-/-}$ (black bar) mice before, 2 and 5 days after doxorubicin (Dox, 20 mg/kg) injection. A: BAX:BCL2 protein ratio and B: Levels of cleaved PARP in the hearts before and 2 days after Dox injection. C: Levels of nitrotyrosine, D: Levels of acetylated p53 acetylation, E: Levels of CXCL1 and F: myeloperoxidase in the hearts before and 5 days after Dox injection. Data (mean ± SEM; n = 5–9 per group) were analyzed by 2-way ANOVA. $^{*}P < .05$, $^{\#}P < .05$ vs. day 0 within the same genotype.

apoptosis and was increased 5 days after Dox injection in both genotypes. However, we observed significantly less p53 acetylation in PAR-$1^{-/-}$ mice compared to PAR-$1^{+/+}$ mice (Fig. 6D). In addition, we measured markers of inflammation, CXCL1 and myeloperoxidase, before and 5 days after Dox injection. Dox injection resulted in increased CXCL1 protein levels in the heart of both genotypes (Fig. 6E). However, PAR-$1^{+/+}$ hearts exhibited much higher levels of CXCL1 after Dox injection compared to PAR-$1^{-/-}$ hearts (Fig. 6E). Furthermore, only PAR-$1^{+/+}$ hearts exhibited increased levels of myeloperoxidase after Dox injection which was higher compared to PAR-$1^{-/-}$ mice hearts (Fig. 6F).

Importantly, PAR-$1^{-/-}$ mice exhibited significantly less cardiac injury in the acute model of Dox-induced cardiotoxicity (Fig. 7A). Furthermore, PAR-$1^{-/-}$ mice had less impairment of cardiac function after Dox administration in both the acute and chronic models compared with PAR-$1^{+/+}$ mice (Fig. 7B and C, Supplement table 1 and Supplement table 2).

4.6. Effect of inhibition of PAR-1 in WT mice treated with Dox

We determined if PAR-1 inhibition in WT mice with vorapaxar was also protective against Dox-induced cardiotoxicity. PAR-$1^{+/+}$ and PAR-$1^{-/-}$ mice were orally gavaged with vorapaxar (30 μg/kg) or vehicle control 1 h before and then daily after Dox injection. Importantly, vorapaxar reduced Dox-induced cardiac impairment of WT mice (Fig. 7D, Supplement table 3). As expected, PAR-$1^{-/-}$ mice had less impairment of cardiac function after Dox treatment compared to WT mice and this was not affected by administration of vorapaxar (Fig. 7D, Supplement Table 3).

5. Discussion

In this study, we identified a pathogenic role of PAR-1 in Dox-induced cardiotoxicity. In vitro experiments revealed that PAR-1 activation enhances Dox-mediated mitochondrial dysfunction in rat and mouse CFs and CMs. The PAR-1-dependent increase in Dox-induced mitochondrial dysfunction was associated with increased ROS and mitochondrial superoxide formation, and apoptosis of CFs and CMs. Consistent with our data, PAR-1 has been shown to activate p53 and increase apoptosis of lung epithelial cells treated with leukocyte elastase [35]. In vivo, we observed an increased BAX:BCL2 protein ratio, PARP cleavage, oxidative stress, and activation of the p53 pathway, as well as increased inflammation in the hearts of PAR-$1^{+/+}$ compared to PAR-$1^{-/-}$ mice after Dox injection. Importantly, PAR-$1^{-/-}$ mice were protected from cardiotoxicity in both acute and chronic Dox-induced heart failure models. In addition, the PAR-1 inhibitor vorapaxar

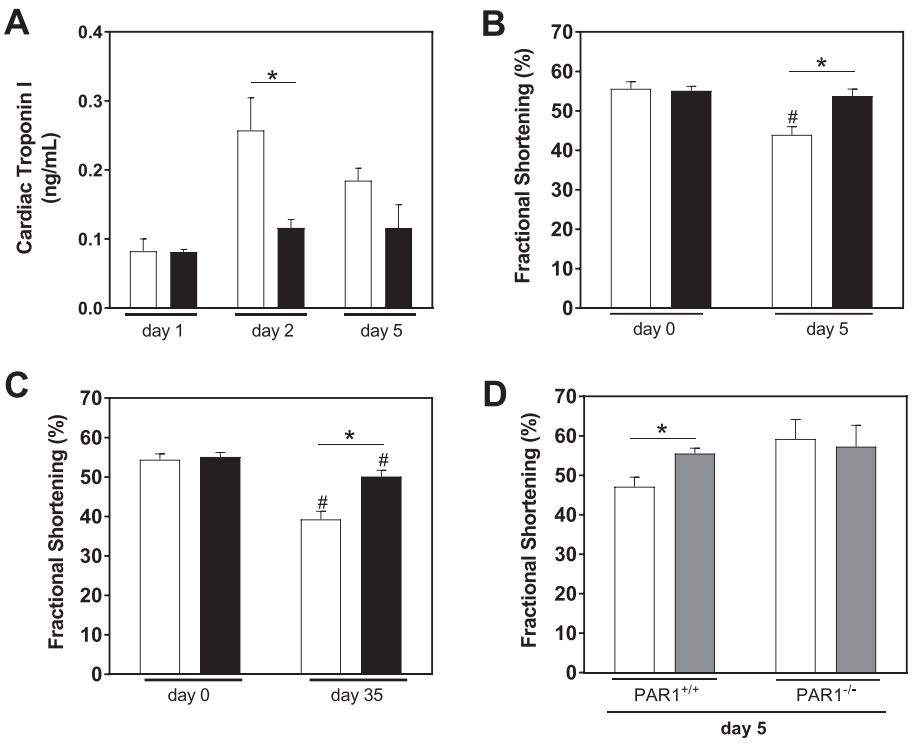

Fig. 7. PAR-1 deficiency and PAR-1 inhibition is associated with reduced cardiac injury and reduced heart failure induced by doxorubicin. A: Cardiac injury was assessed by measuring levels of cardiac troponin I in the plasma from PAR-$1^{+/+}$ (white bar) and PAR-$1^{-/-}$ (black bar) mice at different times after doxorubicin (Dox, 20 mg/kg) injection. B: Echocardiographic analysis of heart function shown as fractional shortening of PAR-$1^{+/+}$ (white bar) and PAR-$1^{-/-}$ (black bar) mice before and 5 days after Dox (20 mg/kg) injection. C: Fractional shortening of mice before and after injection of Dox weekly (5 mg/kg) for 35 days (cumulative dose 25 mg/kg). D: PAR-$1^{+/+}$ and PAR-$1^{-/-}$ mice were treated before and daily after doxorubicin (Dox) injection (20 mg/kg) with vehicle (white bars) or the PAR-1 inhibitor vorapaxar (30 µg/kg, gray bar) by oral gavage. Heart function was measured by echocardiography and shown as fractional shortening at day 5. Data (mean ± SEM; n = 5–9 per group [A-C] and for D: PAR-$1^{+/+}$ $n = 10–12$ and PAR-$1^{-/-}$ $n = 4–5$) were analyzed by 2-way ANOVA. $^{*}P < .05$, $^{\#}P < .05$ vs. day 0 within the same genotype.

reduced Dox-induced cardiotoxicity in WT mice.

We showed that PAR-1 activation contributes to cardiac remodeling and cardiac dysfunction after cardiac injury induced by ischemia-reperfusion injury, as well as treatment with isoproterenol or angiotensin II infusion [11, 13, 21]. In addition, we found that PAR-1 signaling contributes to angiotensin II-induced cardiovascular remodeling and inflammation [13]. Interestingly, inhibition of the angiotensin receptor reduced Dox toxicity in rats and humans, which may be due, in part, to reduced PAR-1 activation [2, 36].

A major finding of our study is that PAR-1 activation enhances Dox-mediated mitochondrial dysfunction and this increases mitochondrial superoxide, ROS and cardiac cell death. In line with our observation, a study showed that PAR-1 stimulation of platelets leads to a loss of ΔΨm due to increased intracellular H_2O_2 generation [37]. Importantly, Dox-induced apoptosis is linked to Ca^{2+}-dependent ROS formation, mitochondrial dysfunction and apoptosis [38, 39]. Here, we showed that Ca^{2+} signaling inhibition abolished the effect of PAR-1 activation on Dox-induced changes in ΔΨm reduction in rat CFs. This suggests that PAR-1 activation enhances pathologic Dox-mediated Ca^{2+} signaling enhancing the toxic feedback cycle of ROS generation and mitochondria injury leading to cell death. Our data are in line with a recent publication, using Q94, an antagonist of PAR-1-dependent Ca^{2+} signaling, in Dox-induced kidney injury [40]. There, the authors linked PAR-1 activation to enhanced Ca^{2+}-dependent oxidative stress and apoptosis in podocytes after treatment with Dox [40].

PAR-1 was shown to enhance the progression of cancer in several models, including breast, colon, prostate, and melanoma [41]. The thrombin–PAR-1 pathway promotes invasion of tumor cells by increasing the secretion of MMPs [42]. Further, PAR-1 can stimulate melanoma cell chemokinesis and metastasis and correlated with the metastatic potential of melanoma cells [43, 44]. Silencing of PAR-1 in these cells reduced tumor growth and metastasis in vivo [45]. In addition, inhibition of thrombin-induced PAR-1 activation by dabigatran etexilate reduced proliferation, migration, and pro-angiogenetic effects of breast and glioblastoma cancer cell lines in vitro and in vivo [46, 47]. Co-treatment with both low dose cyclophosphamide and dabigatran etexilate also led to significantly smaller mammary tumors and fewer lung metastases than mice treated with cyclophosphamide or dabigatran etexilate alone [48].

PAR-1 is the major thrombin receptor on human platelets. Cancer is associated with increased platelet activation [49]. Activated platelets release extracellular vesicles and growth factors that can contribute to tumor proliferation, growth, invasion, and angiogenesis [49]. Interestingly, a PAR-1 polymorphism with increased PAR-1 expression/reactivity was associated with increased tumor progression, relapse and mortality [50]. The effect of PAR-1 inhibition by the FDA-approved PAR-1 inhibitor vorapaxar has not yet been evaluated in cancer patients. However, long-term antiplatelet treatments in the TRITON, TRACER, PEGASUS, DAPT and the APPRAISE-2 trial were linked to an increase of first occurrence of solid cancers in patients with myocardial infarctions. [51] A possible explanation is that “cancer follows bleeding” or more accurately persistent platelet inhibition and/or anticoagulation promoted development and dissemination of early-stage unclassified cancer cells [51]. However, the survival rate of trial patients with newly occurred cancer did not differ compared to a control cohort [51].

Most importantly, we were able to show that vorapaxar treatment of mice improved the heart function to levels seen in PAR-$1^{-/-}$ mice after Dox injection. This suggests that vorapaxar could reduce the cardiotoxic effects of Dox in patients. We did not see any off-target effects of vorapaxar since it had no additional effect in PAR-$1^{-/-}$ mice with regards to the heart function. Our data are highly relevant for the field of cardio-oncology. We found a new therapeutic indication of an already FDA-approved drug which will shorten the time to clinic significantly to improve cancer patients' life.

In conclusion, our study showed that interference with the PAR-1 signaling pathway reduced Dox cardiotoxicity in mice. Dox use is limited due to its cardiotoxicity. Reducing the cardiotoxic effects of chemotherapeutic drugs is an emerging topic in cardio-oncology. Inhibition of pathologic PAR-1 signaling during chemotherapy might be a potential way to improve chemotherapy outcome. Importantly, the beneficial effects of PAR-1 inhibition may extend to the tumor itself. Our data suggest that the PAR-1 inhibitor vorapaxar might be beneficial not only by reducing cardiotoxicity by also by preventing thrombotic

events in cancer patients and having a growth-restricting effect on certain malignant tumors themselves.

Supplementary data to this article can be found online at https://doi.org/10.1016/j.yjmcc.2018.08.008.

Competing interests statement

None.

Acknowledgement

We want to thank Ying Zhang and Alyson C. Auriemma for excellent technical assistance. The study was supported by grants NC TraCS (550KR151602 to S. Antoniak) and the Uehara Memorial Foundation (to K. Tatsumi). The project described was supported by the National Center for Advancing Translational Sciences (NCATS/NIH), through Grant Award Number UL1TR002489. The content is solely the responsibility of the authors and does not necessarily represent the official views of the NIH.

There are no financial interests.

References

[1] E.T. Yeh, H.M. Chang, Oncocardiology-past, present, and future: a review, JAMA Cardiol. 1 (2016) 1066–1072.
[2] C.G. Lenneman, D.B. Sawyer, Cardio-oncology: an update on cardiotoxicity of cancer-related treatment, Circ. Res. 118 (2016) 1008–1020.
[3] J. Liu, W. Mao, B. Ding, C.S. Liang, ERKs/p53 signal transduction pathway is involved in doxorubicin-induced apoptosis in H9c2 cells and cardiomyocytes, Am. J. Physiol. Heart Circ. Physiol. 295 (2008) H1956–H1965.
[4] A. Riad, S. Bien, D. Westermann, P.M. Becher, K. Loya, U. Landmesser, et al., Pretreatment with statin attenuates the cardiotoxicity of doxorubicin in mice, Cancer Res. 69 (2009) 695–699.
[5] L.A. Smith, V.R. Cornelius, C.J. Plummer, G. Levitt, M. Verrill, P. Canney, et al., Cardiotoxicity of anthracycline agents for the treatment of cancer: systematic review and meta-analysis of randomised controlled trials, BMC Cancer 10 (2010) 337.
[6] S. Antoniak, E. Sparkenbaugh, R. Pawlinski, Tissue factor, protease activated receptors and pathologic heart remodelling, Thromb. Haemost. 112 (2014) 893–900.
[7] A. Sabri, J. Short, J. Guo, S.F. Steinberg, Protease-activated receptor-1-mediated DNA synthesis in cardiac fibroblast is via epidermal growth factor receptor transactivation: distinct PAR-1 signaling pathways in cardiac fibroblasts and cardiomyocytes, Circ. Res. 91 (2002) 532–539.
[8] A. Sabri, G. Muske, H. Zhang, E. Pak, A. Darrow, P. Andrade-Gordon, et al., Signaling properties and functions of two distinct cardiomyocyte protease-activated receptors, Circ. Res. 86 (2000) 1054–1061.
[9] U.J. Soh, M.R. Dores, B. Chen, J. Trejo, Signal transduction by protease-activated receptors, Br. J. Pharmacol. 160 (2010) 191–203.
[10] S.F. Steinberg, The cardiovascular actions of protease-activated receptors, Mol. Pharmacol. 67 (2005) 2–11.
[11] R. Pawlinski, M. Tencati, C.R. Hampton, T. Shishido, T.A. Bullard, L.M. Casey, et al., Protease-activated receptor-1 contributes to cardiac remodeling and hypertrophy, Circulation 116 (2007) 2298–2306.
[12] S. Antoniak, R. Pawlinski, N. Mackman, Protease-activated receptors and myocardial infarction, IUBMB Life 63 (2011) 383–389.
[13] S. Antoniak, J.C. Cardenas, L.J. Buczek, F.C. Church, N. Mackman, R. Pawlinski, Protease-activated receptor 1 contributes to angiotensin II-induced cardiovascular remodeling and inflammation, Cardiology 136 (2016) 258–268.
[14] T. Sousou, A.A. Khorana, New insights into cancer-associated thrombosis, Arterioscler. Thromb. Vasc. Biol. 29 (2009) 316–320.
[15] S. Fujihira, T. Yamamoto, M. Matsumoto, K. Yoshizawa, Y. Oishi, T. Fujii, et al., The high incidence of atrial thrombosis in mice given doxorubicin, Toxicol. Pathol. 21 (1993) 362–368.
[16] J.C. Boles, J.C. Williams, R.M. Hollingsworth, J.G. Wang, S.L. Glover, A.P. Owens IIIet al., Anthracycline treatment of the human monocytic leukemia cell line THP-1 increases phosphatidylserine exposure and tissue factor activity, Thromb. Res. 129 (2012) 197–203.
[17] M.B. Wolf, J.W. Baynes, The anti-cancer drug, doxorubicin, causes oxidant stress-induced endothelial dysfunction, Biochim. Biophys. Acta 1760 (2006) 267–271.
[18] E.L. Wilkinson, J.E. Sidaway, M.J. Cross, Cardiotoxic drugs Herceptin and doxorubicin inhibit cardiac microvascular endothelial cell barrier formation resulting in increased drug permeability, Biol. Open 5 (2016) 1362–1370.
[19] S. Antoniak, N. Mackman, Coagulation, protease-activated receptors, and viral myocarditis, J. Cardiovasc. Transl. Res. 7 (2014) 203–211.
[20] S.R. Coughlin, Thrombin signalling and protease-activated receptors, Nature 407 (2000) 258–264.
[21] F. Jaffre, A.E. Friedman, Z. Hu, N. Mackman, B.C. Blaxall, Beta-adrenergic receptor stimulation transactivates protease-activated receptor 1 via matrix metalloproteinase 13 in cardiac cells, Circulation 125 (2012) 2993–3003.
[22] S. Antoniak, A.P. Owens 3rd, M. Baunacke, J.C. Williams, R.D. Lee, A. Weithauser, et al., PAR-1 contributes to the innate immune response during viral infection, J. Clin. Invest. 123 (2013) 1310–1322.
[23] U. Boltzen, A. Eisenreich, S. Antoniak, A. Weithaeuser, H. Fechner, W. Poller, et al., Alternatively spliced tissue factor and full-length tissue factor protect cardiomyocytes against TNF-alpha-induced apoptosis, J. Mol. Cell. Cardiol. 52 (2012) 1056–1065.
[24] L. Gianni, L. Vigano, A. Locatelli, G. Capri, A. Giani, E. Tarenzi, et al., Human pharmacokinetic characterization and in vitro study of the interaction between doxorubicin and paclitaxel in patients with breast cancer, J. Clin. Oncol. Off. J. Am. Soc. Clin. Oncol. 15 (1997) 1906–1915.
[25] S. Antoniak, K. Tatsumi, M. Bode, S. Vanja, J.C. Williams, N. Mackman, Protease-activated receptor 1 enhances poly I:C induction of the antiviral response in macrophages and mice, J. Innate Immun. 9 (2017) 181–192.
[26] S. Antoniak, E.M. Sparkenbaugh, M. Tencati, M. Rojas, N. Mackman, R. Pawlinski, Protease activated receptor-2 contributes to heart failure, PLoS One 8 (2013) e81733.
[27] A.L. Darrow, W.P. Fung-Leung, R.D. Ye, R.J. Santulli, W.M. Cheung, C.K. Derian, et al., Biological consequences of thrombin receptor deficiency in mice, Thromb. Haemost. 76 (1996) 860–866.
[28] V.G. Desai, E.H. Herman, C.L. Moland, W.S. Branham, S.M. Lewis, K.J. Davis, et al., Development of doxorubicin-induced chronic cardiotoxicity in the B6C3F1 mouse model, Toxicol. Appl. Pharmacol. 266 (2013) 109–121.
[29] K. Tatsumi, S. Antoniak, S. Subramaniam, B. Gondouin, S.D. Neidich, M.A. Beck, et al., Anticoagulation increases alveolar hemorrhage in mice infected with influenza A, Phys. Rep. 4 (2016) e13071.
[30] S. Antoniak, M Rojas, D. Spring, T.A. Bullard, E.D. Verrier, B.C. Blaxall, et al., Protease-activated receptor 2 deficiency reduces cardiac ischemia/reperfusion injury, Arterioscler. Thromb. Vasc. Biol. 30 (2010) 2136–2142.
[31] R.D. Olson, P.S. Mushlin, Doxorubicin cardiotoxicity: analysis of prevailing hypotheses, FASEB J. 4 (1990) 3076–3086.
[32] P. Menna, E. Salvatorelli, G. Minotti, Cardiotoxicity of antitumor drugs, Chem. Res. Toxicol. 21 (2008) 978–989.
[33] Y.W. Zhang, J. Shi, Y.J. Li, L. Wei, Cardiomyocyte death in doxorubicin-induced cardiotoxicity, Arch. Immunol. Ther. Exp. 57 (2009) 435–445.
[34] L. Dong, W.W. Xu, H. Li, K.H. Bi, In vitro and in vivo anticancer effects of marmesin in U937 human leukemia cells are mediated via mitochondrial-mediated apoptosis, cell cycle arrest, and inhibition of cancer cell migration, Oncol. Rep. 39 (2018) 597–602.
[35] T. Suzuki, C. Yamashita, R.L. Zemans, N. Briones, A. Van Linden, G.P. Downey, Leukocyte elastase induces lung epithelial apoptosis via a PAR-1-, NF-kappaB-, and p53-dependent pathway, Am. J. Respir. Cell Mol. Biol. 41 (2009) 742–755.
[36] H.F. Sakr, A.M. Abbas, A.Z. Elsamanoudy, Effect of valsartan on cardiac senescence and apoptosis in a rat model of cardiotoxicity, Can. J. Physiol. Pharmacol. 94 (2016) 588–598.
[37] J.J. Lopez, G.M. Salido, J.A. Pariente, J.A. Rosado, Thrombin induces activation and translocation of Bid, Bax and Bak to the mitochondria in human platelets, J. Thromb. Haemost. 6 (2008) 1780–1788.
[38] S.V. Kalivendi, S. Kotamraju, H. Zhao, J. Joseph, B. Kalyanaraman, Doxorubicin-induced apoptosis is associated with increased transcription of endothelial nitric-oxide synthase. Effect of antiapoptotic antioxidants and calcium, J. Biol. Chem. 276 (2001) 47266–47276.
[39] Z. Wang, J. Wang, R. Xie, R. Liu, Y. Lu, Mitochondria-derived reactive oxygen species play an important role in Doxorubicin-induced platelet apoptosis, Int. J. Mol. Sci. 16 (2015) 11087–11100.
[40] Y. Guan, D. Nakano, Y. Zhang, L. Li, W. Liu, M. Nishida, et al., A protease-activated receptor-1 antagonist protects against podocyte injury in a mouse model of nephropathy, J. Pharmacol. Sci. 135 (2017) 81–88.
[41] A.P. Elste, I. Petersen, Expression of proteinase-activated receptor 1-4 (PAR 1-4) in human cancer, J. Mol. Histol. 41 (2010) 89–99.
[42] A.R. Radjabi, K. Sawada, S. Jagadeeswaran, A. Eichbichler, H.A. Kenny, A. Montag, et al., Thrombin induces tumor invasion through the induction and association of matrix metalloproteinase-9 and beta1-integrin on the cell surface, J. Biol. Chem. 283 (2008) 2822–2834.
[43] X. Shi, B. Gangadharan, L.F. Brass, W. Ruf, B.M. Mueller, Protease-activated receptors (PAR1 and PAR2) contribute to tumor cell motility and metastasis, Mol. Cancer Res. 2 (2004) 395–402.
[44] G.J. Villares, M. Zigler, A.S. Dobroff, H. Wang, R. Song, V.O. Melnikova, et al., Protease activated receptor-1 inhibits the Maspin tumor-suppressor gene to determine the melanoma metastatic phenotype, Proc. Natl. Acad. Sci. U. S. A. 108 (2011) 626–631.
[45] V.O. Melnikova, K. Balasubramanian, G.J. Villares, A.S. Dobroff, M. Zigler, H. Wang, et al., Crosstalk between protease-activated receptor 1 and platelet-activating factor receptor regulates melanoma cell adhesion molecule (MCAM/MUC18) expression and melanoma metastasis, J. Biol. Chem. 284 (2009) 28845–28855.
[46] F. Vianello, L. Sambado, A. Goss, F. Fabris, P. Prandoni, Dabigatran antagonizes growth, cell-cycle progression, migration, and endothelial tube formation induced by thrombin in breast and glioblastoma cell lines, Cancer Med. 5 (2016) 2886–2898.
[47] K. DeFeo, C. Hayes, M. Chernick, J.V. Ryn, S.K. Gilmour, Use of dabigatran etexilate to reduce breast cancer progression, Cancer Biol. Ther. 10 (2010) 1001–1008.
[48] E.T. Alexander, A.R. Minton, C.S. Hayes, A. Goss, J. Van Ryn, S.K. Gilmour, Thrombin inhibition and cyclophosphamide synergistically block tumor progression and metastasis, Cancer Biol. Ther. 16 (2015) 1802–1811.
[49] M.Z. Wojtukiewicz, D. Hempel, E. Sierko, S.C. Tucker, K.V. Honn, Thrombin-unique coagulation system protein with multifaceted impacts on cancer and metastasis, Cancer Metastasis Rev. 35 (2016) 213–233.
[50] F.G. Uzunoglu, N. Yavari, B.A. Bohn, M.F. Nentwich, M. Reeh, K. Pantel, et al., C-X-C motif receptor 2, endostatin and proteinase-activated receptor 1 polymorphisms as prognostic factors in NSCLC, Lung Cancer 81 (2013) 123–129.
[51] V.L. Serebruany, A. Tomek, M.H. Kim, Survival after solid cancers in antithrombotic trials, Am. J. Cardiol. 116 (2015) 969–972.